RSC Advances

PAPER

View Article Online
View Journal | View Issue

Cite this: *RSC Adv.*, 2024, **14**, 7258

Received 13th December 2023
Accepted 16th February 2024

DOI: 10.1039/d3ra08519h

rsc.li/rsc-advances

Mechanochromic aromatic hydrocarbons that bear one simple substituent†

Tomohiro Seki * and Kota Hattori

Structurally simple aromatic hydrocarbons that possess only one isocyano group show luminescent mechanochromism. The structural isomers of these aromatic hydrocarbons exhibit blue- and red-shifted emission bands upon mechanical stress. Their low molecular weight enables their sublimation under mild conditions.

Luminescent mechanochromism is a phenomenon that involves an emission-color change in solids or liquid crystals induced by mechanical stimulation such as grinding and pressing.[1–4] Various organic and organometallic compounds have been reported to show luminescent mechanochromism.[5–13] So far, a variety of strategies have been developed to generate mechanochromic compounds, including the use of multiple intermolecular interactions,[7,14,15] connection of donor and acceptor units,[16,17] controlling dipole moments,[18] and switching between monomeric and assembled states.[19] However, these strategies require mechanochromic compounds with rather complicated molecular structures; thus, low-molecular-weight mechanochromic compounds are still scarce.

Polycyclic aromatic hydrocarbons (PAHs) such as anthracene,[20–22] pyrene,[7,23–26] and perylene[27–29] are among the structurally simplest mechanochromic compounds. These PAHs contain a variety of functional substituents, such as amide, cyano, boronic ester, and alkyl groups and/or linkages to other aromatic or heteroaromatic groups. However, except for an unusual example,[30] reports that describe unsubstituted PAHs show luminescent mechanochromism remain elusive. This indicates that the introduction of several substituents or connection to the same or other π-conjugated groups is required to endow simple PAHs with mechanochromic properties. Especially mechanochromic PAHs that bear only one simple substituent remain a rarety.[31]

Here, we report structurally simple monosubstituted pyrene isomers **1** and **4**, which exhibit luminescent mechanochromism. Compared with other reported mechanochromic compounds, the chemical structures of **1** and **4** are relatively simple, *i.e.*, they contain only one isocyano group as a substituent and their molecular weight is low (MW = 227). Solid samples of **1** and **4** exhibit luminescent mechanochromism with blue- and red-shifted emission bands, respectively. X-ray diffraction (XRD) analyses indicated that the ground phase of **1** is a crystalline phase, while that of **4** is an amorphous phase. The crystal structures revealed the presence of moderate dipole–dipole interactions in the ground phases compared to those in their pristine phases, which is the key for the mechanochromism of **1** and **4**.

Pyrene **4** was prepared from 4-nitropyrene according to a previously reported procedure for monoisocyano PAHs (for details, see the ESI†).[32] Pyrene **1**, which has already been reported, was prepared in a similar manner.[33] Although **1** was reported not to show luminescent mechanochromism,[33] we found that both **1** and **4** exhibit luminescent mechanochromic properties.

Under excitation at 365 nm, solid samples of pristine **1** and **4** emit green and blue photoluminescence, respectively (Fig. 1). Crystalline **1** shows an intense green emission with an absolute emission quantum yield (Φ_{em}) of 48% (Table S1†) and an unstructured emission spectrum with a peak at 495 nm (Fig. 2a). Compared with the structured emission of monomeric **1** in CH_2Cl_2 (c = 5 μM, Fig. S1b and S2†), the emission maximum wavelength ($\lambda_{em,max}$) of **1** in the solid state is red-shifted. The average emission lifetime (τ_{av}) of pristine solid **1** is 61 ns, which is longer than that of monomeric **1** in CH_2Cl_2 (13 ns; Fig. S3a and Table S1†). This indicates that the emission of **1** should be characterized as excimer fluorescence.[23,24,34] Meanwhile, pyrene **4** shows blue emission upon photoexcitation (Fig. 1) with an Φ_{em} of 51% (Table S1†) and a broad emission spectrum with a $\lambda_{em,max}$ of 452 nm (Fig. 2b), which is shorter than that of **1**. An emission-decay analysis indicated that the τ_{av} of **4** is 38 ns (Fig. S3b and Table S1†), revealing its excimer character.[23,24,34] The longer $\lambda_{em,max}$ and τ_{av} of the excimer emission of **1** compared with those of **4** could stem from the stronger interactions of **1** in the excited state.[35]

To investigate the difference between the $\lambda_{em,max}$ of pristine **1** and **4**, single-crystal XRD analyses were performed. A single crystal of **1** was obtained from the vapor-diffusion method using $CHCl_3$ and *n*-pentane. Compound **1** crystallizes in the triclinic $P\bar{1}$

Department of Chemistry, Faculty of Science, Shizuoka University, Shizuoka 422-8017, Japan. E-mail: seki.tomohiro@shizuoka.ac.jp

† Electronic supplementary information (ESI) available: X-ray crystallographic data, optical-microscopy images, thermal data, emission spectra, and other additional information. CCDC 2312583. For ESI and crystallographic data in CIF or other electronic format see DOI: https://doi.org/10.1039/d3ra08519h

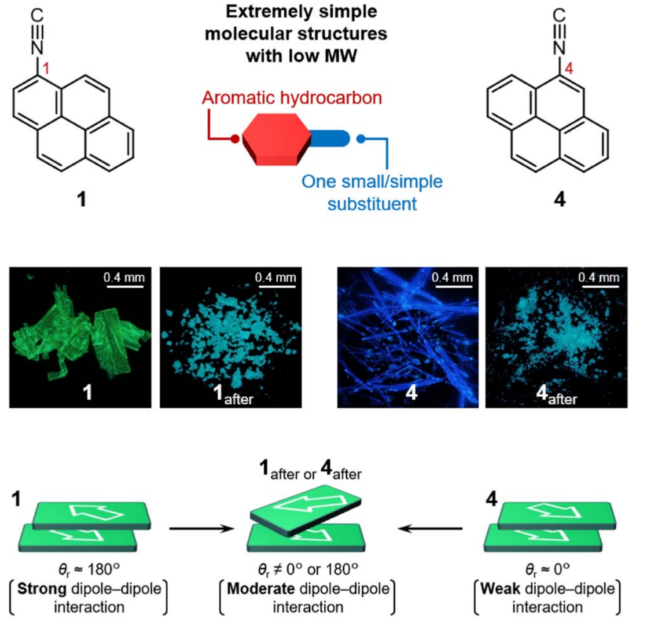

Fig. 1 Chemical structures of **1** and **4**. Photographs of **1**, $\mathbf{1}_{\mathrm{after}}$, **4**, and $\mathbf{4}_{\mathrm{after}}$ taken under UV light ($\lambda_{\mathrm{ex}} = 365$ nm). Schematic representation of stacked dimers of **1**, $\mathbf{1}_{\mathrm{after}}$, **4**, and $\mathbf{4}_{\mathrm{after}}$. Rotation angles of the dipoles of the molecules within the dimer are depicted as θ_{r}.

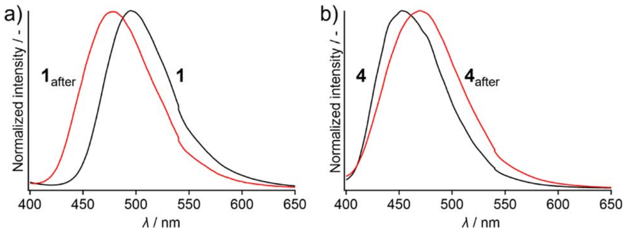

Fig. 2 Emission spectra of solid samples of (a) **1** and $\mathbf{1}_{\mathrm{after}}$ and (b) **4** and $\mathbf{4}_{\mathrm{after}}$ upon excitation at 365 nm.

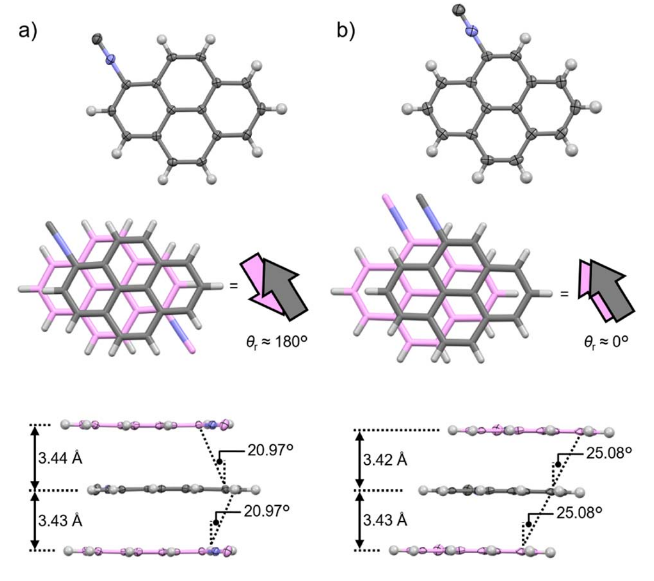

Fig. 3 Molecular structures of (a) **1** and (b) **4** in the single crystal.

space group (Fig. 3a and S5 as well as Table S2†).[33] As typically observed for the crystal structures of flat π-systems,[36,37] **1** adopts a co-facial stacking arrangement in a head-to-tail manner with a rotational angle of the isocyano groups (θ_{r}) of ~180° (Fig. 3a). These molecules form a one-dimensional (1D) column with an offset along the long axis of the pyrene core (20.97°; Fig. 3a and S5†) and a short distance of ~3.44 Å between the pyrene cores. Single crystals of **4** were also obtained using the vapor-diffusion method with $CHCl_3$ and *n*-pentane. Compound **4** crystallizes in the monoclinic $P2_1/c$ space group (Fig. 3b and S6 as well as Table S2†) and also adopts a stacking arrangement to form a column with a longitudinal offset along the molecular long axis (25.08°; Fig. 3b and S6†) similar to that of **1**. However, head-to-head arrangements ($\theta_{\mathrm{r}} \approx 0°$) within the column were confirmed for **4** despite the presence of the electron-withdrawing isocyano group (the dipole moment of **4** was estimated to be 4.41 D *via* DFT calculations; Fig. S7†). However, the stacking distance between molecules of **4** is relatively short (~3.43 Å), which is almost identical to that of **1** with $\theta_{\mathrm{r}} \approx 180°$. Thus, the dipole moment of **4** should be cancelled out along the *bc* plane, *i.e.*, orthogonal to the stacking direction (Fig. S8†).

The different stacking arrangements of **1** (head-to-tail) and **4** (head-to-head) are most likely responsible for their different $\lambda_{\mathrm{em,max}}$. Considering that the π-stacking distance and offset angles within the co-facial 1D columns of **1** (3.44 Å and 20.97°, respectively) and **4** (3.43 Å and 25.08°, respectively) are close, a similar degree of excimer formation would be expected. However, the $\lambda_{\mathrm{em,max}}$ of **1** (495 nm) is longer than that of **4** (452 nm), which can be attributed to the stronger dipole–dipole interactions of the former as revealed by its head-to-tail arrangement ($\theta_{\mathrm{r}} \approx 180°$). Indeed, structurally simple anthracene molecules have been reported to show longer wavelength emission when excimer formation is assisted by dipole–dipole interactions within the stacked dimers.[37] The stronger excimer-like character for the emission of **1** compared to that of **4** is supported by the longer emission lifetime of the former compared to that of the latter (Fig. S3 and Table S1†).

Upon grinding, the emission band of **1** was blue-shifted whereas that of **4** was red-shifted. Upon applying mechanical stimulation using a spatula, the emission color of **1** changed from green to light blue (Fig. 1). The resulting powder, $\mathbf{1}_{\mathrm{after}}$, showed a broad emission band with a $\lambda_{\mathrm{em,max}}$ of 478 nm (Fig. 2a). Such a blue-shifted emission induced by grinding is less common for luminescent mechanochromic compounds[38,39] than a corresponding red-shifted emission. The ground powder of $\mathbf{1}_{\mathrm{after}}$ showed an Φ_{em} of 37% and an τ_{av} of 45 ns, indicating excimer-emission character (Fig. S9a and Table S3†).[23,24,34] In contrast, when pristine **4** was mechanically ground, a red-shifted emission band was observed (Fig. 2b). The ground powder of **4** ($\mathbf{4}_{\mathrm{after}}$) showed light-blue emission (Fig. 1) with an Φ_{em} of 33% and an τ_{av} of 31 ns (Fig. S9b and Table S3†). This long emission lifetime was attributed to excimer emission.[23,24,34] The emission spectrum of $\mathbf{4}_{\mathrm{after}}$ is broad and has a maximum at 470 nm, similar to that of $\mathbf{1}_{\mathrm{after}}$ ($\lambda_{\mathrm{em,max}} = 478$ nm; Fig. 2).

Importantly, we confirmed that unsubstituted pyrene molecules exhibit no mechanochromic properties (Fig. S10†), indicating that the introduction of the single isocyano group endows **1** and **4** with mechanochromic properties.

Powder XRD (PXRD) analyses indicated that $\mathbf{1}_{\mathrm{after}}$ forms a crystalline phase, while $\mathbf{4}_{\mathrm{after}}$ forms an amorphous phase. The PXRD patterns of $\mathbf{1}_{\mathrm{after}}$ and $\mathbf{4}_{\mathrm{after}}$ were compared with those simulated for the corresponding pristine phases derived from the single-crystal coordinates. The simulated pattern of **1** shows three intense diffraction peaks at 9.40°, 10.93°, and 12.10° (black line in Fig. 4a). After applying stress for a short time, new crystalline peaks appeared at 9.47°, 11.31°, and 12.35°, while the original diffraction peaks of **1** remained as shoulders (yellow line in Fig. 4a). This result implies the coexistence of two different crystalline structures of **1** in an intermediate state.[40] After thorough grinding, the residual shoulders derived from the pristine molecular arrangement disappeared (red line in Fig. 4a), suggesting that the mechanochromism of **1** is based on a crystal-to-crystal phase transition, which is an uncommon phase transition for mechanochromic compounds.[9,13,25,41,42] Conversely, upon mechanical stimulation of **4**, the intensity of the diffraction peaks (*i.e.*, $2\theta = 10°–12°$) of pristine **4** (black line in Fig. 4b) decreased significantly in ground $\mathbf{4}_{\mathrm{after}}$ and no new diffraction peaks emerged (red line in Fig. 4b). This result indicates that a crystal-to-amorphous phase transition is the origin of the mechanochromism of **4**, which is typically observed for this class of materials.[8–12,15–17,21,28,39,43,44]

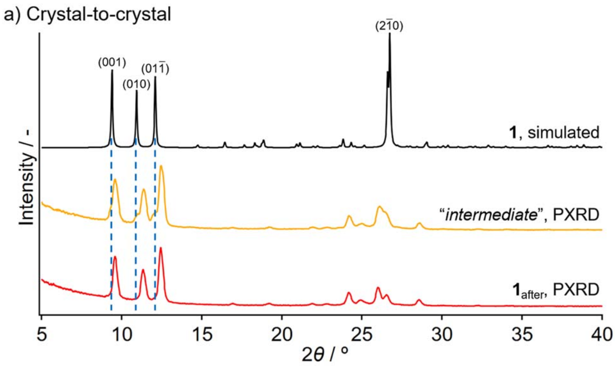
a) Crystal-to-crystal

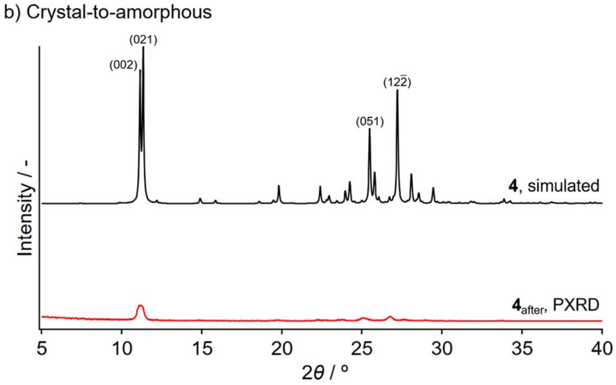
b) Crystal-to-amorphous

Fig. 4 Simulated PXRD patterns of pristine forms derived from the single-crystal structures (black lines) and experimental PXRD patterns of the ground powders (red lines) of (a) **1** and (b) **4**. The yellow line in (a) is the PXRD pattern of the "intermediate" sample of **1**, which was obtained from grinding for a short time. Miller indices are shown for four intense diffraction peaks of the simulated powder patterns of **1** and **4**.

In ground-phase $\mathbf{1}_{\mathrm{after}}$ and $\mathbf{4}_{\mathrm{after}}$, "moderate" dipole–dipole interactions might be formed compared to pristine **1** and **4**. As mentioned above, the dipole–dipole interactions along the stacking direction in the crystalline phases of **1** and **4** are strong and weak, respectively, as reflected in their corresponding θ_{r} values (∼180° for **1** and ∼0° for **4**). These extreme θ_{r} values of the unground phases should become moderate ($\theta_{\mathrm{r}} \neq 0°$ or 180°) upon phase transition into the ground phases irrespective of the crystalline ($\mathbf{1}_{\mathrm{after}}$) or amorphous phases ($\mathbf{4}_{\mathrm{after}}$, Fig. 5). This result indicates that the dipole–dipole interactions are most likely weakened after the phase transition from **1** and strengthened from **4** in terms of θ_{r} upon grinding (Fig. 5). This is consistent with the blue-shifted emission of **1** and the red-shifted emission of **4**. Generally, in addition to θ_{r}, dipole–dipole interactions are also affected by the torsional angles and distance between the π planes relative to the stacking direction (Fig. S11†).[45] However, the lack of a detailed crystal-structure analysis for unknown crystalline $\mathbf{1}_{\mathrm{after}}$ and amorphous $\mathbf{4}_{\mathrm{after}}$ at this stage hindered unveiling the effect of the torsional angles and distances on the emission wavelength.

Upon thermal treatment, pristine **1** and **4** exhibited a similar behavior to that induced by mechanical stimulation. Thus, heating a pristine solid sample of **1** to 100 °C resulted in an emission-color change from green to light blue (Fig. S12a†). The resulting light-blue emission of **1** remained intact upon cooling to room temperature (Fig. S12a†). The light-blue-emitting crystals of **1** can be regarded as $\mathbf{1}_{\mathrm{after}}$ because their emission spectrum and PXRD patterns are similar to those of $\mathbf{1}_{\mathrm{after}}$ obtained from mechanical stimulation (Fig. S12b and S12c†). Differential-scanning-calorimetry (DSC) studies of **1** confirmed a thermal phase-transition temperature of 100 °C (Fig. S13 and S14†).[46] Similar to **1**, a solid sample of **4** showed thermoresponsive behavior similar to that observed upon mechanical stimulation, *i.e.*, thermo-induced amorphization of **4** led to a red-shifted emission band (Fig. S15†). These results indicate that mechanical stimulation and thermal treatment induce the same phase transitions in **1** and **4**, leading to clear luminescent chromic behavior.

Compounds **1** and **4** are the luminescent mechanochromic compounds with one of the lowest molecular weights (MW = 227) reported to date.[47] Accordingly, we expected that it should be possible to sublime **1** and **4** under mild conditions,

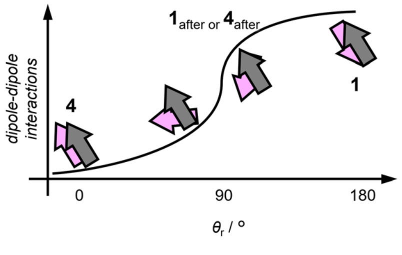

Fig. 5 Schematic representation of the relationship of θ_{r} within the co-facial arrangements of the dipoles (depicted by arrows) in the stacked dimer and the strength of the dipole–dipole interactions.

potentially enabling the low-cost preparation of thin films. To confirm this hypothesis, we conducted preliminary sublimation experiments. After placing a solid sample of **1** in a round bottom flask and reducing the pressure to 2.5 mbar while slowly increasing the temperature, sublimation started at 40 °C (Fig. S16a†). ^{1}H NMR and polarized-optical-microscopy analyses confirmed that the sublimated solid is **1**, *i.e.*, **1** did not undergo decomposition and maintained crystallinity (Fig. S16b and S17†).[48] A similar result was observed for pyrene **4**, *i.e.*, sublimation occurred at 2.5 mbar and 50 °C (Fig. S18 and S19†). Such mild sublimation conditions (moderate pressure/low temperature) might enable the cost-efficient preparation of large thin films. A more detailed analysis of the sublimation properties, *i.e.*, determination of the vapor pressure, and preparation of thin films with a single domain of **1** and **4** will be the subject of future work.

Conclusions

We have reported that structurally simple pyrene molecules **1** and **4**, which bearing only one small isocyano group, exhibit luminescent mechanochromism. Upon exposure to mechanical stress, **1** showed a blue-shifted emission band as a result of a crystal-to-crystal phase transition, while **4** exhibited a red-shifted emission as a result of amorphization. The crystal-structure analyses of **1** and **4** indicated that the change in the strength of the dipole–dipole interactions with neighboring molecules is the origin of their opposite emission-color changes. The low molecular weight of these compounds enables their sublimation under mild conditions (2.5 mbar and 40–50 °C). This study thus offers a new molecular-design strategy to obtain mechanochromic compounds based on the connection of one aromatic core and one small substituent.

Author contributions

TS designed the project; KH performed and analyzed the experiments with guidance from TS; TS wrote the manuscript.

Conflicts of interest

There are no conflicts to declare.

Acknowledgements

This work was financially supported by JSPS KAKENHI grants JP22H021550 and JP22K190580 as well as JST, PRESTO grant JPMJPR21AB (Japan).

Notes and references

1 Z. Chi, X. Zhang, B. Xu, X. Zhou, C. Ma, Y. Zhang, S. Liu and J. Xu, *Chem. Soc. Rev.*, 2012, **41**, 3878–3896.

2 Y. Sagara and T. Kato, *Nat. Chem.*, 2009, **1**, 605–610.

3 Y. Sagara, S. Yamane, M. Mitani, C. Weder and T. Kato, *Adv. Mater.*, 2016, **28**, 1073–1095.

4 S. Xue, X. Qiu, Q. Sun and W. Yang, *J. Mater. Chem. C*, 2016, **4**, 1568–1578.

5 S. Mataka, H. Moriyama, T. Sawada, K. Takahashi, H. Sakashita and M. Tashiro, *Chem. Lett.*, 1996, **25**, 363–364.

6 S. Mizukami, H. Houjou, K. Sugaya, E. Koyama, H. Tokuhisa, T. Sasaki and M. Kanesato, *Chem. Mater.*, 2005, **17**, 50–56.

7 Y. Sagara, T. Mutai, I. Yoshikawa and K. Araki, *J. Am. Chem. Soc.*, 2007, **129**, 1520–1521.

8 H. Ito, T. Saito, N. Oshima, N. Kitamura, S. Ishizaka, Y. Hinatsu, M. Wakeshima, M. Kato, K. Tsuge and M. Sawamura, *J. Am. Chem. Soc.*, 2008, **130**, 10044–10045.

9 T. Seki, Y. Takamatsu and H. Ito, *J. Am. Chem. Soc.*, 2016, **138**, 6252–6260.

10 M. Jin, T. Seki and H. Ito, *Chem. Commun.*, 2016, **52**, 8083–8086.

11 B. Huitorel, H. E. Moll, M. Cordier, A. Fargues, A. Garcia, F. Massuyeau, C. Martineau-Corcos, T. Gacoin and S. Perruchas, *Inorg. Chem.*, 2017, **56**, 12379–12388.

12 B. Huitorel, R. Utrera-Melero, F. Massuyeau, J. Mevelec, B. Baptiste, A. Polian, T. Gacoin, C. Martineau-Corcos and S. Perruchas, *Dalton Trans.*, 2019, **48**, 7899–7909.

13 Z. Wang, F. Yu, W. Chen, J. Wang, J. Liu, C. Yao, J. Zhao, H. Dong, W. Hu and Q. Zhang, *Angew. Chem., Int. Ed.*, 2020, **59**, 17580–17586.

14 S. J. Yoon and S. Y. Park, *J. Mater. Chem.*, 2011, **21**, 8338–8346.

15 T. Seki, K. Kobayashi, T. Mashimo and H. Ito, *Chem. Commun.*, 2018, **54**, 11136–11139.

16 R. Yoshida, T. Tachikawa and S. Ito, *Cryst. Growth Des.*, 2021, **22**, 547–558.

17 T. Ishi-i, H. Tanaka, R. Kichise, C. Davin, T. Matsuda, N. Aizawa, I. S. Park, T. Yasuda and T. Matsumoto, *Chem.–Asian J.*, 2021, **16**, 2136–2145.

18 S. Yagai, S. Okamura, Y. Nakano, M. Yamauchi, K. Kishikawa, T. Karatsu, A. Kitamura, A. Ueno, D. Kuzuhara, H. Yamada, T. Seki and H. Ito, *Nat. Commun.*, 2014, **5**, 4013.

19 T. Seki, N. Tokodai, S. Omagari, T. Nakanishi, Y. Hasegawa, T. Iwasa, T. Taketsugu and H. Ito, *J. Am. Chem. Soc.*, 2017, **139**, 6514–6517.

20 Y. Sagara, S. Yamane, T. Mutai, K. Araki and T. Kato, *Adv. Funct. Mater.*, 2009, **19**, 1869–1875.

21 P. Xue, B. Yao, X. Liu, J. Sun, P. Gong, Z. Zhang, C. Qian, Y. Zhang and R. Lu, *J. Mater. Chem. C*, 2015, **3**, 1018–1025.

22 H. Tanikubo, T. Matsuo and S. Hayashi, *Bull. Chem. Soc. Jpn.*, 2023, **96**, 178–182.

23 T. Wang, N. Zhang, K. Zhang, J. Dai, W. Bai and R. Bai, *Chem. Commun.*, 2016, **52**, 9679–9682.

24 E. Nagata, T. Ara and H. Nakano, *Dyes Pigm.*, 2017, **141**, 48–52.

25 Q. Kong, W. Zhuang, G. Li, Y. Xu, Q. Jiang and Y. Wang, *New J. Chem.*, 2017, **41**, 13784–13791.

26 X. Su, Y. Ji, W. Pan, S. Chen, Y.-M. Zhang, T. Lin, L. Liu, M. Li, Y. Liu and S. X.-A. Zhang, *J. Mater. Chem. C*, 2018, **6**, 6940–6948.

27 F. Donati, A. Pucci, C. Cappelli, B. Mennucci and G. Ruggeri, *J. Phys. Chem. B*, 2008, **112**, 3668–3679.

28 N. Mizoshita, T. Tani and S. Inagaki, *Adv. Mater.*, 2012, **24**, 3350–3355.

29 M. P. Aldred, G.-F. Zhang, C. Li, G. Chen, T. Chen and M.-Q. Zhu, *J. Mater. Chem. C*, 2013, **1**, 6709–6718.

30 Unsubstituted anthracene shows luminescent mechanochromism only at low temperature; for details, see: F. Kannen, M. Nishimura, K. Yoza and T. Kusukawa, *Tetrahedron*, 2023, **149**, 133710.

31 Pyrene molecules with one bis(pinacolato)diboryl or alkoxycarbonyl group represent another simple molecular design for luminescent mechanochromism; for details, see: ref. 23 and 25.

32 K. Kato, T. Seki and H. Ito, *Inorg. Chem.*, 2021, **60**, 10849–10856.

33 X. Y. Wang, J. Zhang, J. Yin and S. H. Liu, *Chem.–Asian J.*, 2019, **14**, 2903–2910.

34 Y. Sagara, T. Muramatsu and N. Tamaoki, *Crystals*, 2019, **9**, 92.

35 Similar to the emission spectra, the solid-state UV-vis absorption spectra of **1** has the onset and peak at a longer wavelength compared to those of **4** (Fig. S4). This could be due to the stronger intermolecular interactions of the former relative to the latter even in the ground state.

36 S. K. Rajagopal, A. M. Philip, K. Nagarajan and M. Hariharan, *Chem. Commun.*, 2014, **50**, 8644–8647.

37 A. M. Philip, S. K. Manikandan, A. Shaji and M. Hariharan, *Chem.–Eur. J.*, 2018, **24**, 18089–18096.

38 T. Seki, K. Kashiyama and H. Ito, *Dalton Trans.*, 2019, **48**, 7105–7109.

39 T. Seki and D. Korenaga, *Chem.–Eur. J.*, 2023, **29**, e202302333.

40 The coexistence of two different molecular arrangements in **1** is supported by the observed “intermediate” powder sample prepared by heating (Fig. S12c).

41 T. Seki, K. Sakurada and H. Ito, *Chem. Commun.*, 2015, **51**, 13933–13936.

42 M. Jin, T. Seki and H. Ito, *J. Am. Chem. Soc.*, 2017, **139**, 7452–7455.

43 P. Xue, J. Sun, P. Chen, P. Wang, B. Yao, P. Gong, Z. Zhang and R. Lu, *Chem. Commun.*, 2015, **51**, 10381–10384.

44 Z. Lin, X. Mei, E. Yang, X. Li, H. Yao, G. Wen, C.-T. Chien, T. J. Chow and Q. Ling, *CrystEngComm*, 2014, **16**, 11018–11026.

45 F. Würthner, *Acc. Chem. Res.*, 2016, **49**, 868–876.

46 Unfortunately, the single-crystal X-ray diffraction analysis of a thermally obtained crystal of $\mathbf{1}_{\text{after}}$ was inconclusive, most likely due to the proximity of the thermal phase-transition temperature of 1 (100 °C) to its melting point (130 °C; Fig. S13).

47 For structurally simple luminescent pyrene molecules without mechanochromc properties, see: ref. 36. For mechanochromic compounds with low molecular weight (MW = 218–271), see: refs. 16, 43, and 44.

48 Under these conditions, the single crystallinity of the sublimated samples of **1** could not be confirmed.